HOW GOOD ARE THE FITS TO THE EXPERIMENTAL VELOCITY PROFILES *IN VIVO* ?

Aristotle G. KOUTSIARIS [1,3,*], Sophia V. TACHMITZI [2], Athanassios D. GIANNOUKAS [3]

* Corresponding author: Tel.: ++30 (2410) 555278; Fax: ++30 (2410) 555378; Email: ariskout@otenet.gr
1: Bioinformatics Lab, Dept of Medical Labs, Technological Educational Institute of Larissa, Greece
2: Ophthalmology Department, General Hospital of Larissa, Greece
3: Department of Vascular Surgery, University of Thessaly, Larissa, Greece

Abstract A new velocity profile equation for the description of microcirculatory blood flow *in vivo* was proposed in 2009. However various recently published papers still use the assumption of parabolic velocity profile (Poiseuille flow). The purpose of this work was to evaluate the performance of 3 different fitting cases: **1)** best parabolic fit, **2)** axial fit with the proposed equation and **3)** best fit with the proposed equation. Twelve experimental velocity profiles measured by particle image velocimetry in mouse venules were used to compare the fitting efficiency of the 3 cases on the basis of the velocity relative error (RE) expressed as average ± SE (standard error) at ten different radial segments (REj with $1 \leq j \leq 10$). The parabolic best fit (**case 1**) leads to serious deviations from the real velocity distribution (RE_{10} = - 65% ± 2%). The proposed equation axial fit (**case 2**) slightly overestimates blood velocity distribution near the vessel wall but the <REj> was below + 12% and it requires only one experimental value near the vessel axis, measurable using the Doppler Effect. The proposed equation best fit (**case 3**) approximates the experimental data without any serious bias but requires a complete velocity profile data set.

Keywords: Microcirculation, Fits, Velocity Profiles, *In Vivo*

1. Introduction

In the case of non-Newtonian fluids, such as blood, the velocity profile inside cylindrical tubes is considerably blunter than a parabolic profile. However, a lot of researchers working in the areas of blood flow inside *in vitro* models (Chen and Sharp 2010, Liang et al 2009) or inside blood vessels *in vivo* (Ibrahim and Berk 2009, Nagaoka and Yoshida 2006, Seki et al 2004) still use the parabolic velocity profile (Poiseuille flow).

This may be a consequence of the use of well-known Newtonian fluids to evaluate the performance of new measuring techniques (Kuang et al 2009, Lima et al 2006). Lima et al (2006) experimented also with low hematocrit (10%) blood which tends to behave like a Newtonian fluid.

It should be emphasized that the velocity profile is crucial in the analytical estimation of other important hemodynamic parameters such as the volume flow and wall shear rate.

A new velocity profile equation for the description of microcirculatory blood flow *in vivo* was proposed in 2009 (Koutsiaris 2009). The purpose of this work was to evaluate the performance of 3 different fitting cases: **1)** best parabolic fit, **2)** axial fit with the proposed equation and **3)** best fit with the proposed equation. The fitting efficiency was quantified using the criterion of the velocity relative error, on original particle image velocimetry data from mice (Long et al 2004).

2. Methods

2.1 The velocity profile equations

The general form of the 2 velocity profile equations is presented bellow:

$$V_p(r) = V_m \left[1 - \left(\frac{r}{R} \right)^2 \right] \qquad (1)$$

$$V_K(r) = V_m \left[1 - \kappa_1 \left(\frac{r}{R}\right)^2\right]\left[1 - \left(\frac{r}{R}\right)^{\kappa_2}\right] \quad (2)$$

Where $V_p(r)$ and $V_\kappa(r)$ are the velocities at radial position r, for the parabolic and the proposed equation respectively, R is the radius of the cylindrical vessel, V_m is the maximum velocity of the symmetrical analytical profile on the vessel axis and κ_1 and κ_2 are parameters affecting the velocity profile shape.

The second equation describes a velocity profile blunter than the parabolic, with the same V_m, when the following conditions are satisfied: $0 < \kappa_1 < 1$, $\kappa_2 > 2$ and $(1-\kappa_1)\,\kappa_2 \geq 2$.

2.2 Velocity profile data

In contrast to a previous work where the velocity data point coordinates were estimated graphically (Koutsiaris 2009), here, twelve original velocity profile data were used from the mouse cremaster muscle (Long et al 2004). The velocity profiles were measured by particle image velocimetry in venules ranging in diameter between 21 and 39 μm.

2.3 Fits

The best fits for the parabolic (case 1) and the proposed equation (case 3) were estimated from the experimental profiles using nonlinear regression analysis (SPSS 18).

For the axial fit (case 2), the κ parameters in the second equation must be replaced by static values. Taking as a fact that the average ratio of the measured wall shear rate (WSR) over the parabolic WSR is 4.6, the parameters κ_1 and κ_2 of the proposed equation can be estimated as equal to 0.58 and 22 respectively (Koutsiaris 2009).

2.4 Evaluation criteria

The fitting efficiency was evaluated on the basis of the velocity relative error (RE) as percentage (%) of the real values.

A velocity profile equation V(r) approximates each experimental velocity point to a certain degree. This approximation can be quantified by the velocity relative error (RE):

$$RE(r) = \frac{V(r) - \text{Experimental Value}}{\text{Experimental Value}} 100\% \quad (3)$$

Depending on the velocity profile equation and the fitting technique, the RE changes along the vessel radius in a different way. To see how the average RE (< RE >) of all the 12 experimental profiles changes along the vessel radius, for the 3 aforementioned fitting cases, the relative error was expressed as average ± SE (standard error) at ten different radial segments (REj with $1 \leq j \leq 10$, Fig 1).

3. Results

In each radial segment j, the average and standard error of the velocity relative error RE ($< RE >_j$ and RE_{SEj} respectively) of all the 12 profiles was estimated.

The < RE > of the parabolic equation best fit **(case 1),** presented with gray columns in figure 1, reached a maximum negative value of - 65% at j = 10. The parabolic best fit tends to overestimate the real velocity of blood near the vessel axis (RE_1 = + 14% ± 3% (RE_{SE1})) and to underestimate severely the real velocity near the vessel wall (RE_8 = - 20% ± 2%, RE_9 = - 41% ± 2% and RE_{10} = - 65% ± 2%). The RE_{SE} of the parabolic equation best fit, for all radial positions j, was less than 3.5%.

The < RE > of the proposed equation axial fit **(case 2),** presented with columns filled with diagonal lines in figure 1, reached a maximum positive value of + 11% at j = 8 and at j = 9. The proposed equation axial fit tends to overestimate the real velocity of blood near the wall (RE_8 = + 11% ± 3%, RE_9 = + 11% ± 5% and RE_{10} = + 5% ± 5%). The RE_{SE} of the second case for all radial positions j, was less than 5%.

The < RE > of the proposed equation best fit **(case 3),** presented with white columns in figure 1, ranged between – 1% and + 2%. There are no severe biases and the RE_{SE} for all radial positions j, was less than 2%.

4. Discussion

A preliminary comparison was performed between 2 different velocity profile equations: the classic parabolic equation and a recently proposed equation (Koutsiaris 2009). The comparison intended to test their suitability in describing the real velocity profile of venular blood *in vivo*.

From a practical point of view, the axial fit of the proposed equation (case 2) presents the greatest interest, since the blood velocity measurement near the vessel axis seems to be a simple task in the laboratory and the clinical environment, using the Doppler Effect.

According to the results shown in Fig. 1, the < RE > of the proposed equation axial fit did not exceed the absolute value of 11% at any of the radial segments. In contrast, the parabolic equation best fit (case 1) showed an increasing average negative bias towards the vessel wall, up to the value of – 65%.

A graphical presentation of the 3 fitting cases, together with an actual velocity profile data set from a 36.6 μm mouse venule (Long et al 2004) are shown in Fig. 2.

The blood flow in the mouse venules was considered to be steady, axisymmetric and fully developed (Long et al 2004). Even though the velocity pulse is significant in the precapillary arterioles of mammals (Koutsiaris & Pogiatzi 2004, Koutsiaris et al 2010), it should be almost completely attenuated in cremaster muscle venules with diameters higher than 20μm for the following reasons.

First, in the capillaries, due to their small diameters and their usual change of direction, significant pulse attenuation occurs. An example of this attenuation is shown in Fig.3, in a rabbit mesenteric capillary with internal diameter of 7 microns (Koutsiaris et al 2000).

Second, the capillaries in muscle tissue are expected to be much longer than the capillaries in a tissue with low metabolic demands like the mesentery.

Third, the diameters of the post capillary mouse venules should be in the range between 10 to 15 μm. This is at least one venular order lower than the mouse venules with diameters between 20 and 40 μm used in the study of Long et al (2004).

The considerable blunting of the velocity profile of blood is a logical consequence of the shear thinning non-Newtonian properties of this biological fluid. At low shear rates, increased viscosity values are observed due to microstructural changes in the fluid (Kaliviotis et al 2010). At any flow inside a cylindrical geometry, the lowest shear is observed on the axis. Therefore, the increased viscosity near the axis contributes to the blunting of the velocity profile.

Even though the second equation was initially proposed for small mammals, there is no strong argument against its use to humans. Human blood viscosity and red blood cell aggregation are considerably higher than in small mammals, at very low shear rates (shear rates < 10 s^{-1}). According to equation 2, these low shear rates appear at radial positions less than ≈ 18% of the microvessel radius R, where the velocity profile is already very blunt.

Therefore it seems logical to assume that in physiologic cases, aggregative and viscous phenomena would not affect drastically the velocity profile of blood and that the same equation with the axial fit technique could be used in humans.

Acknowledgements

We wish to thank Professor E.R. Damiano (Boston University, USA) for sending the necessary experimental data.

References

Chen, Y and Sharp, M.K., 2011. A strain-based flow-induced hemolysis prediction model calibrated by in vitro erythrocyte deformation parameters. Artif. Organs 35(2), 145-156.

Ibrahim, J and Berk, B.C., 2009. Flow-mediated vascular remodeling in hypertension: relation to hemodynamics. Stroke 40(2), 582-590.

Kaliviotis, E., Dusting J., Balabani S., 2010. Spatial Variation of blood viscosity: Modelling using shear fields measured by a μPIV based technique. Medical Engineering & Physics, in press.

Koutsiaris, A.G., Pogiatzi, A., Tsangaris, S., 2000. Velocity measurements and wall shear stress estimation in the mesenteric microvasculature of frogs and rabbits. International Journal of Cardiovascular Medicine and Science 3(1), 39-48.

Koutsiaris, A.G. and Pogiatzi, A., 2004. Velocity pulse measurements in the mesenteric arterioles of rabbits. Physiol. Meas. 25, 15-25.

Koutsiaris, A.G., 2009. A velocity profile equation for blood flow in small arterioles and venules of small mammals *in vivo* and an evaluation based on literature data. Clinical Hemorheology and Microcirculation 43, 321-334.

Koutsiaris, A.G., Tachmitzi, S.V., Papavasileiou, P., Batis, N., Kotoula, M., Giannoukas, A.D., Tsironi, E., 2010. Blood velocity pulse quantification in the human conjunctival pre-capillary arterioles. Microvascular Research 80, 202-208.

Kuang, C., Zhao, W., Yang, F., Wang, G., 2009. Measuring flow velocity distribution in microchannels using molecular tracers. Microfluid Nanofluid 7, 509-517.

Liang, S., Hoskins, M., Dong, C., 2009. Tumor cell extravasation by leukocyte adhesion is shear rate dependent on IL-8 signaling. Mol. Cell Biomech. 7(2), 77-91.

Lima, R., Wada, S., Tsuboda, K., Yamaguchi, T., 2006. Confocal micro-PIV measurements of three-dimensional profiles of cell suspension flow in a square microchannel. Meas. Sci. Technol. 17, 797-808.

Long, D.S., Smith, M.L., Pries, A.R., Ley, K., Damiano, E.R., 2004. Microviscometry reveals reduced blood viscosity and altered shear rate and shear stress profiles in microvessels after hemodilution. PNAS 101, 10060-10065.

Nagaoka, T. and Yoshida, A., 2006. Noninvasive Evaluation of Wall Shear Stress on Retinal Microcirculation in Humans. Invest. Ophthalmol. Vis. Sci. 47(3), 1113-1119.

Seki, J., Satomura, Y., Ooi, Y., 2004. Velocity pulse advances pressure pulse by close to 45^0 in the rat pial arterioles. Biorheology 41, 45-52.

FIGURE CAPTIONS

Fig. 1. The average value of the velocity relative error RE for all the experimental profiles, at each radial segment j, is shown with columns. Grey columns represent the parabolic best fit (case 1). Columns filled with diagonal lines and white columns represent the proposed equation axial fit (case 2) and the best fit (case 3) respectively. The standard error of the mean is shown with black bars on each column.

Fig. 2. The experimental velocity profile data from a 36.6 μm mouse venule (Long *et al* 2004), with their radial position normalized, are shown in black dots. The parabolic best fit (case 1) is shown in squares. The proposed velocity profile axial fit (case 2) and the best fit (case 3), are shown in triangles and solid black line, respectively.

Fig. 3. Blood velocity pulse attenuation in a rabbit mesenteric capillary with internal diameter of 7 μm (from Koutsiaris et al 2000). Successive velocity measurements in the capillary entrance, at 131 prames per second, are shown in rectangles (the time interval of 21 frames is equivalent to one cardiac cycle). Similar measurements, but 20 capillary diameters downstream, are shown in circles.

FIGURE 1

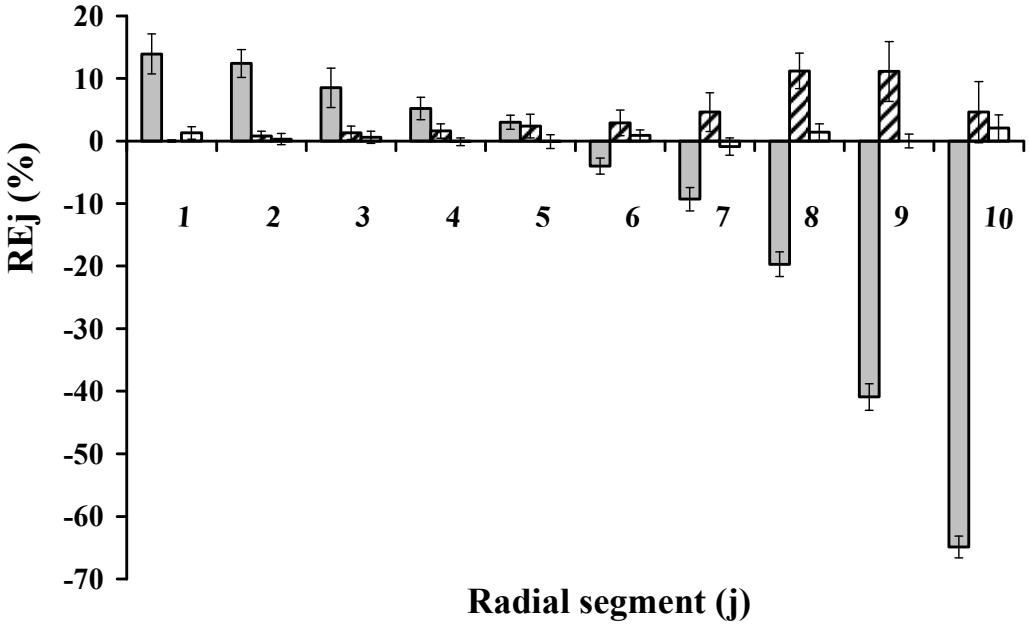

FIGURE 2

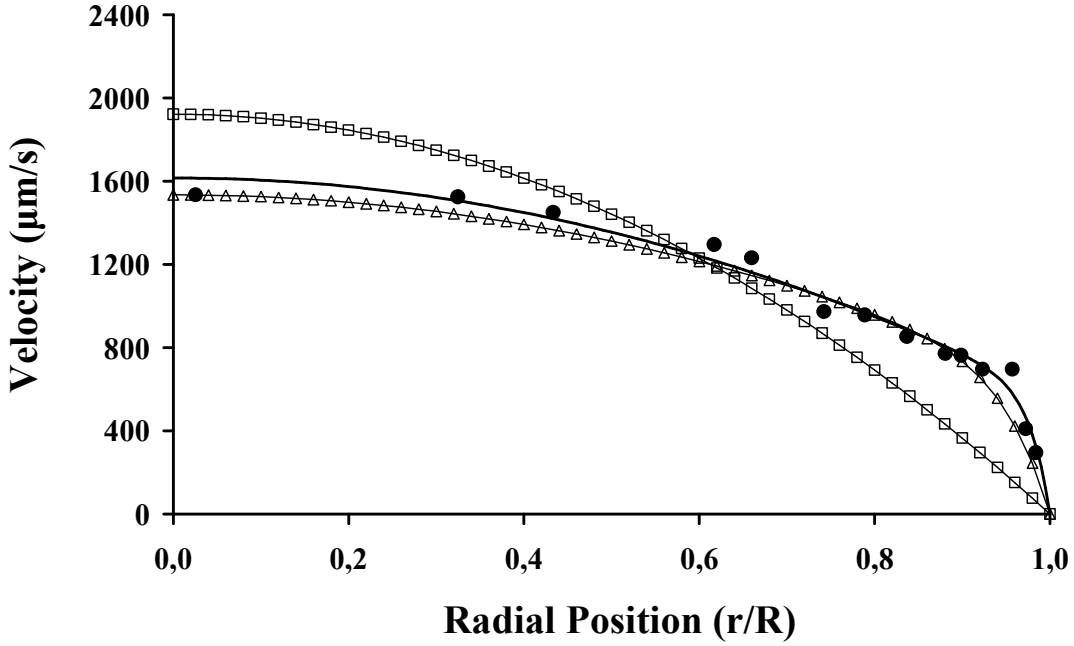
2400
2000
1600
1200
800
400
0
Velocity (µm/s)
0,0
0,2
0,4
0,6
0,8
1,0
Radial Position (r/R)

FIGURE 3

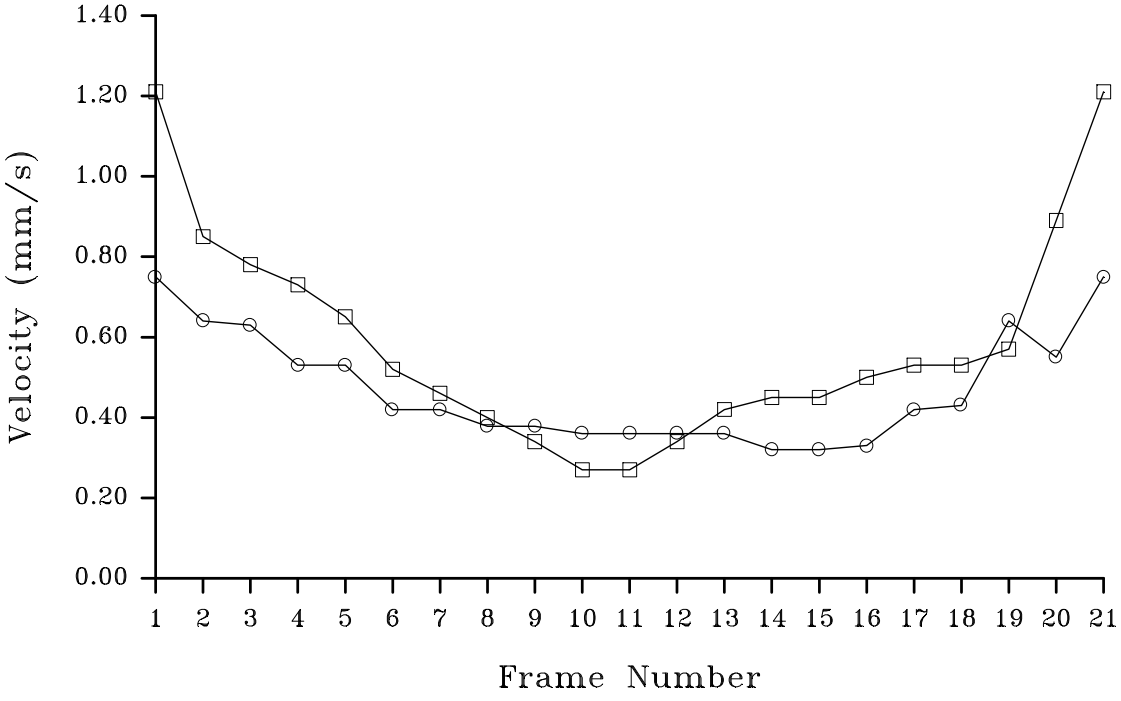
Velocity (mm/s)
1.40
1.20
1.00
0.80
0.60
0.40
0.20
0.00
1 2 3 4 5 6 7 8 9 10 11 12 13 14 15 16 17 18 19 20 21
Frame Number